Quantum Transport Effects in Nanosized Graphite Sheets. II. Enhanced Transport Effects by Heteroatoms

Tomofumi Tada and Kazunari Yoshizawa*

Institute for Materials Chemistry and Engineering, Kyushu University, Fukuoka 812-8581, Japan

Received: July 25, 2002; In Final Form: June 3, 2003

Quantum transport effects in various nanosized graphite sheets are studied on the basis of the Landauer model. To derive heteroatomic effects in quantum transport, nanosized graphite sheets that involve B, N, and O atoms are treated. Important rules for effective quantum transport are found: (I) two atoms connected with metallic leads should have large molecular orbital (MO) coefficients in the frontier orbitals (i.e., the highest occupied MO (HOMO) and the lowest unoccupied MO (LUMO) or other MOs in the vicinity of the Fermi energy); (II) the product of MO coefficients at the two atoms should be different in sign between the HOMO and LUMO, and the product of MO coefficients at the two atoms should be same in sign between the HOMO (LUMO) and other occupied (unoccupied) orbitals near the Fermi energy. Heteroatoms are useful to enhance quantum transport effects because heteroatoms in nanosized graphite sheets can decrease the energy gaps and localize the π-electronic populations at certain sites in the HOMO and LUMO.

Introduction

Since a concept of molecular device was proposed by Aviram and Ratner,[1] the characterization of molecular wires that are accessible to single molecular systems is an important issue in nanotechnology. Quantum transport effect is a significant feature in nanosized systems. Landauer's formulation[2] is of great use in evaluating the conductance of molecular wire; several important mechanisms that determine fundamental aspects of the conductance have been derived.[3−12] In the Landauer formalism with Green's function techniques combined with density functional theory, it was reported that the conductance of a molecular wire composed of a fullerene and carbon nanotubes can be controlled by changing the orientation of the fullerene around the cylinder axis of the carbon nanotubes.[6] The Green function method has been extensively used in the issue of electron transfer, and the possibility of using the energy of the transmitted electron as a control parameter in electron-transfer reactions was studied by Ratner et al.[13] In a previous paper,[14] we derived an interesting relationship between the molecular orbitals (MOs) and the conductance of a nanosized graphite sheet including zigzag and armchair edge sites. The localized states that appear on the zigzag edge sites in the nanosized graphite sheet play an important role in effective quantum transport. From tight-binding calculations of graphite ribbons,[15−20] the significance of the zigzag edge in controlling the band gap has been confirmed. Müllen et al. reported systematic syntheses of nanosized graphite sheets through the intermolecular [4 + 2] Diels−Alder reactions.[21] The edges in nanosized graphite sheets synthesized through the Diels−Alder reactions are of almost armchair type. In this paper, we describe quantum transport effects in molecular wires composed of two gold chains and several nanosized graphite sheets, the edges of which consist of almost armchair structures, and derive heteroatomic effects in quantum transport.

* To whom correspondence should be addressed. E-mail: kazunari@ms.ifoc.kyushu-u.ac.jp.

Method of Calculation

To represent quantum transport effects in a molecular wire, we employed the Pariser−Parr−Pople[22] (PPP) Hamiltonian and the formulation for tunneling current by Caroli and Combescot.[23] Because in this treatment all π-electrons are included in the estimation of the electronic structures of molecular wires, intrinsic features of quantum transport effects in π-aggregates will be derived. To verify this treatment, we also employed the ab initio Hartree−Fock (HF) method with the formulation for tunneling current. Let us consider a molecular wire composed of a nanosized graphite sheet and two gold chains. Chart 1 represents nanosized graphite sheets used in our molecular wire models, where the fundamental graphite sheet is $C_{72}H_{26}$ (**1**).[21a] Figure 1A shows a schematic representation of the molecular wire composed of **1** and two gold chains aligned perpendicularly to the graphite plane. In the Caroli−Combescot−Landauer (CCL) formulation within the PPP framework, the Hamiltonian can be written as

$$H = H_0 + H' \tag{1}$$

where

$$H_0 = \sum_{i\in \mathrm{NG}} \left(U_i + \frac{1}{2} P_{ii}\gamma_{ii} + \sum_{j\neq i} (P_{jj} - Z_j)\gamma_{ij} \right) c_i^+ c_i + \sum_{i,j\in \mathrm{NG}} \left(\beta_{ij} - \frac{1}{2} P_{ij}\gamma_{ij} \right) c_i^+ c_j + \sum_{i,j\in \mathrm{GC}} \beta_{ij}^{\mathrm{Au}} c_i^+ c_j \tag{2}$$

and

$$H' = \sum_{\substack{i\in \mathrm{NG} \\ j\in \mathrm{GC}}} \beta_{ij}^{\mathrm{T}} c_i^+ c_j + \sum_{\substack{i\in \mathrm{GC} \\ j\in \mathrm{NG}}} \beta_{ij}^{\mathrm{T}} c_i^+ c_j \tag{3}$$

Here H_0 represents the system in which a nanosized graphite (NG) is infinitely separated from the gold chains (GC), and H' is a term that represents interactions between NG and GC in the molecular wire shown in Figure 1A. The parameters used

10.1021/jp021739t CCC: $25.00
Published on Web 08/06/2003

CHART 1

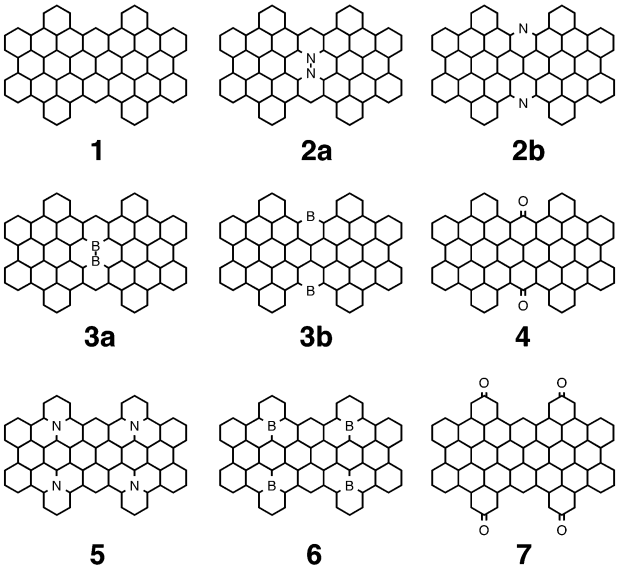

in this model are as follows: U_i is the ionization energies of atoms, C (−11.16 eV), N (−28.59 eV), O (−17.70 eV), and B (−8.30 eV),[24] and the resonance integrals β_{ij} are estimated with the Wolfsberg−Helmholz formula.[25] Z_j is the charge of the core of the j-th atom, and **P** is the density matrix of π-electrons. The one-center, two-electron integrals γ_{ii} are taken from the ionization energies and electron affinities for carbon (γ_{CC} = 11.13 eV), nitrogen (γ_{NN} = 16.63 eV), oxygen (γ_{OO} = 15.23 eV), and boron (γ_{BB} = 7.97 eV).[24] The two-center integrals γ_{ij} are obtained from the one-center integrals.[22] According to surface physics studies, the local density of states (LDOS) of fcc gold is dominated by the s-orbital in the vicinity of the Fermi energy; the LDOS of the s-orbital is about 0.07/(eV atom).[26] Thus, we used β^{Au} = −3.5 eV, which leads to the LDOS of the s-orbital of gold. In the contact sections between the gold chains and the nanosized graphite sheets (**1**−**7**), we used the carbon−gold integral (β^{T}_{C-Au} = 0.4 eV), the nitrogen−gold integral (β^{T}_{N-Au} = 0.2 eV), the oxygen−gold integral (β^{T}_{O-Au} = 0.1 eV), and the boron−gold integral (β^{T}_{B-Au} = 0.7 eV).[27] We obtained the geometries of the nanosized graphite sheets from semiempirical calculations at the AM1 level of theory.[28]

In the CCL formulation within the ab initio HF framework, we used the HF/6-31G(d) method to obtain the electronic states and geometries of nanosized graphite sheets and used the HF/LANL2DZ method for the LDOS of gold. The ab initio HF calculations were carried out with the Gaussian 98 program.[29]

When atoms α and α′ in the gold chains are connected at atoms r and s of a graphite sheet, respectively, the conductance in the zero-temperature limit is written as

$$g_{rs} = \frac{2e^2}{h} T_{rs}(E_F) \tag{4}$$

and

$$T_{rs}(E) = \frac{(2\pi\beta^{T}_{r\alpha}\beta^{T}_{s\alpha'})^2}{2} G^{A}_{sr}(E) G^{R}_{rs}(E) \rho_{\alpha}(E) \rho_{\alpha'}(E) \tag{5}$$

where G^A and G^R are advanced and retarded Green's functions, and ρ_α is the LDOS value at the contact gold atom indicated by α. According to ref 23, the Green's function G is nearly proportional to the 0-th Green's function $G^{(0)}$ obtained in the noninteracting system of a graphite sheet and the gold chains. The relationship between G and $G^{(0)}$ is given as

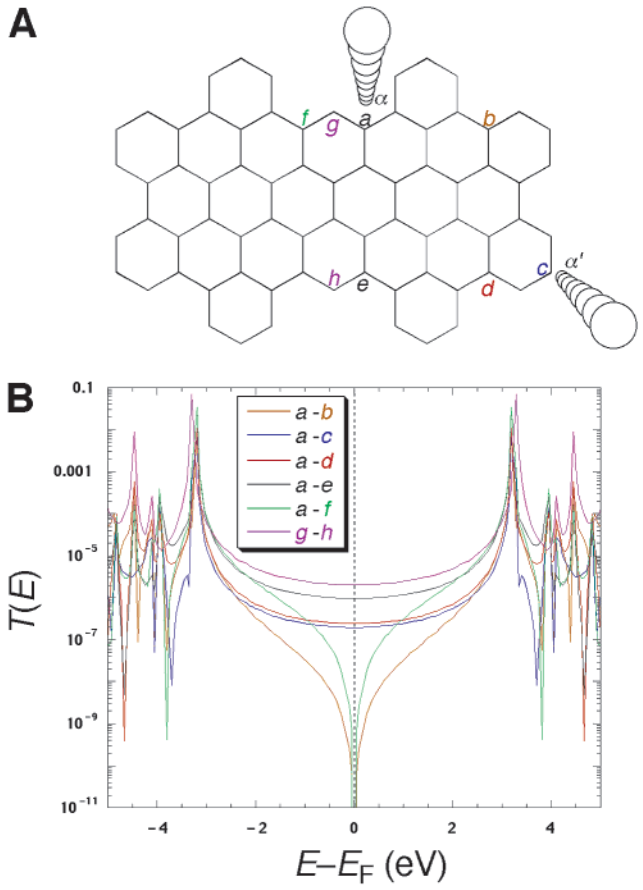

Figure 1. A schematic representation (A) of a molecular wire composed of $C_{72}H_{26}$ and two gold chains. The indices, a, b, ..., h represent carbon atoms that are connected with the terminal gold atoms, α and α′, in the gold chains. Panel B shows the computed transfer coefficients between two atoms in $C_{72}H_{26}$. The curve of a−b corresponds to T_{ab}.

$$G^{R/A}_{rs} = \frac{G^{(0)R/A}_{rs}}{D^{R/A}} \tag{6}$$

and

$$D^{R/A} = \{1 - (\beta^{T}_{r\alpha})^2 G^{(0)R/A}_{rr} G^{(0)R/A}_{\alpha\alpha}\}\{1 - (\beta^{T}_{s\alpha'})^2 G^{(0)R/A}_{ss} G^{(0)R/A}_{\alpha'\alpha'}\} - (\beta^{T}_{r\alpha})^2 (\beta^{T}_{s\alpha'})^2 G^{(0)R/A}_{rs} G^{(0)R/A}_{sr} G^{(0)R/A}_{\alpha\alpha} G^{(0)R/A}_{\alpha'\alpha'} \tag{7}$$

The 0-th Green's function $G^{(0)}$ has the following form:

$$G^{(0)R/A}_{rs}(E) = \sum_k \frac{C_{rk} C^{*}_{sk}}{E - \epsilon_k \pm i\eta} \tag{8}$$

where C_{rk} is the k-th MO coefficient at atom r, ϵ_k is the k-th MO energy of a graphite sheet, and the following equation that describes the relationship between the LDOS and the 0-th Green's function determines the infinitesimal η.

$$\rho_j(E) = -\frac{1}{\pi} \mathrm{Im}\, G^{(0)R}_{jj}(E) \tag{9}$$

Equation 5 indicates that the transfer coefficient T between atoms r and s does not depend on G_{tu} (t and u mean atoms

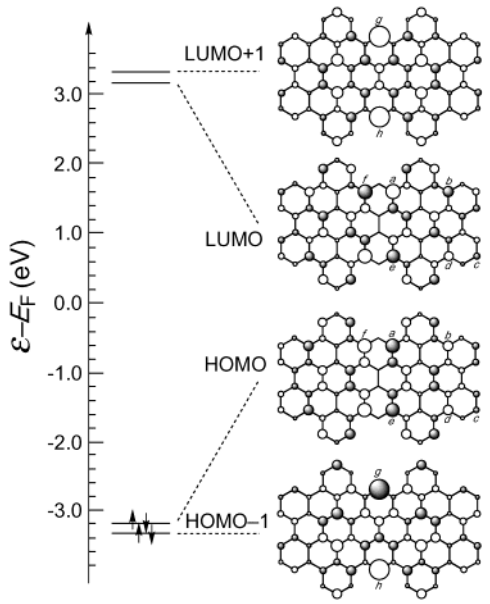

Figure 2. An orbital energy diagram near the Fermi level and the HOMO − 1, HOMO, LUMO, and LUMO + 1 of $C_{72}H_{26}$. The size of a circle on each carbon reflects the π-atomic orbital population.

except for *r* and *s* in a graphite sheet). We think that a key in effective quantum transport between two atoms is the magnitude of MO coefficients at the two atoms.

Results and Discussion

Quantum Transport Effects in $C_{72}H_{26}$ in the CCL Formulation within the PPP Framework. Computed transfer coefficients, *T*s, between two carbon atoms in **1** are shown in Figure 1B. *T*s are sharp ($T = 0.1-0.001$) near the MO energies of **1** (see eq 8). In Figure 1B, T_{ac}, T_{ad}, T_{ae}, and T_{gh} give large coefficients, and T_{ab} and T_{af} give small coefficients at the Fermi energy. Thus, the conductance of the molecular wire significantly depends on how the gold chains are connected with **1**. This variation is characterized by looking at the MOs near the Fermi level because the contribution of such MOs in eq 8 plays a great role in Green's function at the Fermi level. This is similar to the MO interaction concept written in terms of second-order perturbation theory.[30,31]

Figure 2 shows the highest occupied MO (HOMO), the lowest unoccupied MO (LUMO), HOMO − 1, and LUMO + 1 of **1**. The size of each circle corresponds to the population of π-electron, and the solid and open circles show the sign of MO coefficient *C*. The relationship of *T*s in magnitude is explained qualitatively by looking at the HOMO and LUMO. In view of T_{ab}, T_{ac}, T_{ad}, T_{ae}, and T_{af}, it is reasonable that significant quantum transport occurs between the two carbon atoms that have large electronic populations in the HOMO and LUMO (i.e., $T_{ae}(E_F) > T_{ad}(E_F) > T_{ac}(E_F)$). As given in eq 8, magnitude of Green's function depends not only on the energy differences $E - \epsilon_k$ but also on the products of MO coefficients CC^*. At the Fermi energy, the signs of $E_F - \epsilon_{HOMO}$ and $E_F - \epsilon_{LUMO}$ are different in general. Therefore, if the sign of $C_{r_{HOMO}}C^*_{s_{HOMO}}$ is equal to the sign of $C_{r_{LUMO}}C^*_{s_{LUMO}}$, G_{rs} becomes small because the contributions from the HOMO and LUMO are canceled. This cancellation occurs in $T_{ab}(E_F)$ and $T_{af}(E_F)$ (see Figures 1B and 2). Consequently, the sequence of the transfer coefficients (i.e., $T_{ae}(E_F) > T_{ad}(E_F) > T_{ac}(E_F) \gg T_{ab}(E_F)$, $T_{af}(E_F)$) is reasonable from the MO coefficients in the HOMO and LUMO. However, T_{gh} is large although the HOMO and LUMO have no orbital amplitude at atoms g and h. This significant result comes from the HOMO − 1 and LUMO + 1 that lie energetically close to the HOMO and LUMO. The most important feature in the HOMO − 1 and LUMO + 1 is that the π-electronic populations are localized at atoms g and h. This orbital feature results in large $G_{gh}(E_F)$, leading to effective quantum transport between atoms g and h. This significant consequence in **1** is derived from the zigzag edges in the vicinity of atoms g and h. It has been reported that the π-electron localization on the zigzag edges causes graphene to be a weak metal, so this result is reasonable.[19,20]

TABLE 1: Computed Transfer Coefficients at the Fermi Level and Energy Gaps in $C_{72}H_{26}$ (1), $C_{70}N_2H_{26}$ (2a, 2b), $C_{70}B_2H_{26}$ (3a, 3b), and $C_{72}O_2H_{24}$ (4)

	$T(E_F)$ (10^{-6})				
molecule	$T_{11'}$	$T_{22'}$	$T_{33'}$	$T_{44'}$	E_g (eV)
1	2.01[a]	0.96	0.11		6.38
2a	15.79	1.35	0.18		4.15
2b	0.18[b]	5.03	0.39		4.73
3a[c]	1.58	0.43	0.03		6.30
3b	23.83[d]	0.35	0.03		6.07
4	0.27	6.00	0.42	0.01[e]	5.05

[a] This transfer coefficient is identical to the largest one, T_{gh}, in Figure 1. [b] The transfer coefficient between the two nitrogen atoms. [c] The largest transfer coefficient is obtained between the two boron atoms and is calculated to be 1.8×10^{-4}. [d] The transfer coefficient between the two boron atoms. [e] The transfer coefficient between the two oxygen atoms.

The discussion made above is summarized as follows: (I) Atoms A and B the MO coefficients of which are large in the frontier orbitals (i.e., the HOMO and LUMO or other MOs in the vicinity of the Fermi energy) are efficient as connecting sites with metallic leads; (II) the sign of $C_{A_{HOMO}}C^*_{B_{HOMO}}$ must be different from the sign of $C_{A_{LUMO}}C^*_{B_{LUMO}}$ to obtain effective quantum transport in a molecular wire. We expect from these rules that a nanosized graphite sheet in which the electronic population is localized at certain atoms in the HOMO and LUMO can show significant quantum transport. To acquire enhanced quantum transport, we considered nanosized graphite sheets including heteroatoms, $C_{70}N_2H_{26}$ (**2a**, **2b**), $C_{70}B_2H_{26}$ (**3a**, **3b**), $C_{72}O_2H_{24}$ (**4**), $C_{68}N_4H_{26}$ (**5**), $C_{68}B_4H_{26}$ (**6**), and $C_{72}O_4H_{22}$ (**7**), as shown in Chart 1.

Enhanced Quantum Transport Effects in the CCL Formulation within the PPP Framework. Although there are many ways of connection between two atoms in nanosized graphite sheets, we are able to predict important atoms for effective quantum transport by looking at the MOs in the vicinity of the Fermi energy. Computed transfer coefficients between important two atoms in **1**, **2a**, **2b**, **3a**, **3b**, and **4** are listed in Table 1. The connection at atoms 1 and 1′ in **1** leads to the largest transfer coefficient among possible combinations of two atoms in **1**. The HOMOs and LUMOs of **2a**, **3b**, and **4** are depicted in Figure 3, and except for the HOMO of **3b**, the HOMOs and LUMOs are more localized in the central region than those of **1**. We expect that the localized populations and decreased energy gaps will result in enhanced transfer coefficients (e.g., $T_{11'}$ in **2a** and **3b** in Table 1). In a similar manner, $T_{22'}$ in **2b** becomes slightly larger than $T_{11'}$ in **1**. The degree of enhancement in quantum transport corresponds to the π-electronic populations in the HOMO and the LUMO; For example, in $C_{70}N_2H_{26}$ (**2a**), the relation of electronic populations $\tilde{\rho}_{11'} > \tilde{\rho}_{22'} > \tilde{\rho}_{33'}$ in the LUMO corresponds to the relation of transfer coefficients $T_{11'} > T_{22'} > T_{33'}$ (see Figure 3B and Table 1), where $\tilde{\rho}_{rs}$ means the sum of the π-electronic populations at atoms *r* and *s*. In $C_{70}B_2H_{26}$ (**3b**), large quantum transport $T_{11'}$ is obtained despite the zero population in the HOMO at atoms 1 and 1′

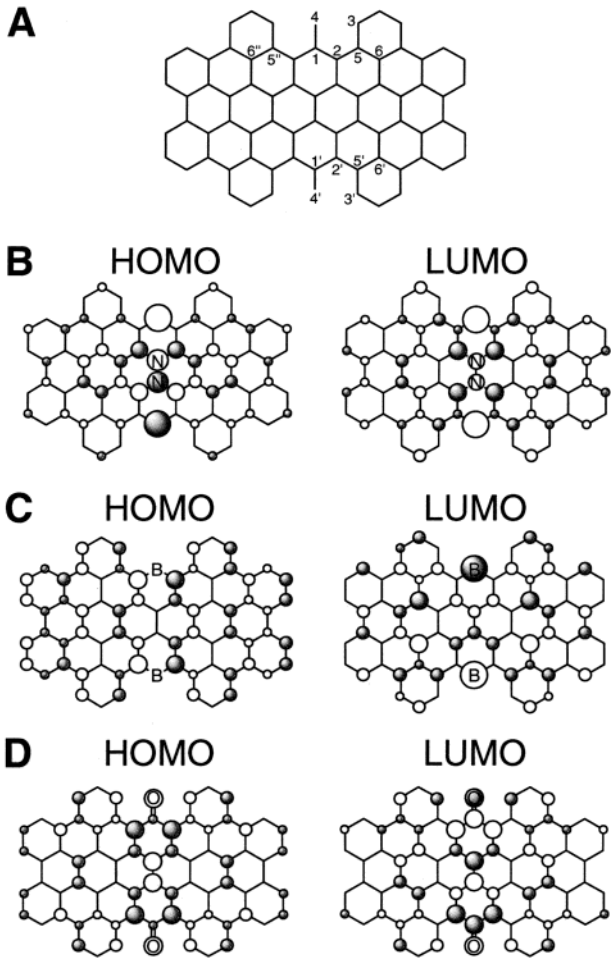

Figure 3. The numerical indices (A) of atoms in nanosized graphite sheets including heteroatoms and are the HOMO and the LUMO in (B) $C_{70}N_2H_{26}$ (**2a**), (C) $C_{70}B_2H_{26}$ (**3b**), and (D) $C_{72}O_2H_{24}$ (**4**). The size of a circle on each atom reflects the π-atomic orbital population.

TABLE 2: Computed Transfer Coefficients at the Fermi Level and Energy Gaps in $C_{68}N_4H_{26}$ (5), $C_{68}B_4H_{26}$ (6), and $C_{72}O_4H_{22}$ (7)

	$T(E_F)$ (10^{-6})					
molecule	$T_{11'}$	$T_{55'}$	$T_{55''}$	$T_{66'}$	$T_{66''}$	E_g (eV)
5	1.68	4.36	45.98	0.18[a]	1.21[a]	2.19
6	1.01	0.06	0.09	2.54[b]	0.14[b]	5.78
7	0.87	0.00	0.00	13.27	0.00	3.93

[a] The transfer coefficient between two nitrogen atoms. [b] The transfer coefficient between two boron atoms.

(i.e., two boron atoms) because the large resonance integral, $\beta^T_{B-Au} = 0.7$ eV, strengthens the contribution from the LUMO in the estimation of transfer coefficient in eq 5. Similarly, large MO coefficients in the LUMO exist at the two boron atoms in **3a**. Thus, we expect that quantum transport should be enhanced by connecting the two boron atoms with metallic leads, and the transfer coefficient $T_{boron-boron}$ is, in fact, estimated to be 1.8×10^{-4} in **3a**. On the other hand, the small resonance integral $\beta^T_{O-Au} = 0.1$ eV results in a decreased transfer coefficient $T_{44'}$ in **4**. However, the two oxygen atoms in **4** lead to the large π-electronic populations at the central sites in the HOMO and the LUMO of **4**, and we therefore expect the enhanced transfer coefficient $T_{22'}$ in **4**.

We computed transfer coefficients in **5**, **6**, and **7** in several ways of connection and summarized those in Table 2. We can predict the locations of efficient connecting sites in view of the frontier orbitals. Figure 4 shows the HOMO, HOMO − 1, LUMO, and LUMO + 1 in **5**; according to rules I and II, the connections at atoms 5 and 5′ and atoms 5 and 5″ are important. However, the transfer coefficient in the connection at atoms 5 and 5′ is not as large as to be expected, while $T_{55''}$ is significantly enhanced. This result derives from the contributions of the HOMO − 1 and LUMO + 1. The MO coefficients in the HOMO − 1 of **5** at atoms 5 and 5′ are as large as those in the HOMO, and thus the contribution from the HOMO − 1 in the summation in eq 8 is significant. Because the Fermi energy does not exist between the HOMO and HOMO − 1, the signs of two denominators in eq 8, $E_F - \epsilon_{HOMO}$ and $E_F - \epsilon_{HOMO-1}$, are the same. Therefore to obtain a significant 0-th Green's function, the product of MO coefficients at two atoms connecting metallic leads should be the same in sign between the HOMO and HOMO − 1. Similarly, the product of MO coefficients at the two atoms should be the same in sign between the LUMO and LUMO + 1. Because the product of MO coefficients at atoms 5 and 5′ in **5** is different in sign between the HOMO (LUMO) and HOMO − 1 (LUMO + 1), the transfer coefficient $T_{55'}$ in **5** does not become very large. On the other hand, the product of MO coefficients at atoms 5 and 5″ is same in sign between the HOMO (LUMO) and HOMO − 1 (LUMO + 1), and therefore, the transfer coefficient $T_{55''}$ is effectively enhanced. Because this rule belongs to rule II, we improved rule II as follows: the product of MO coefficients at the two atoms connecting metallic leads should be different in sign between the HOMO and LUMO, and the product of MO coefficients at the two atoms should be same in sign between the HOMO (LUMO) and the other occupied (unoccupied) orbitals in the vicinity of the Fermi energy.

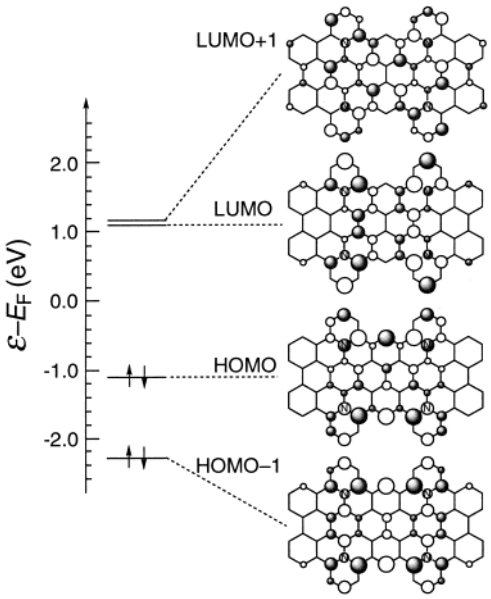

Figure 4. An orbital energy diagram near the Fermi level and the HOMO − 1, HOMO, LUMO, and LUMO + 1 of $C_{68}N_4H_{26}$ (**5**). The size of a circle on each carbon reflects the π-atomic orbital population.

We confirmed by using the CCL formulation within the PPP framework that the HOMOs and LUMOs of nanosized graphite sheets are localized at certain sites by the presence of heteroatoms and as a consequence quantum transport will be enhanced.

Quantum Transport Effects in the CCL Formulation within the ab Initio HF Framework. To confirm the heteroatomic effects derived with the CCL formulation within the PPP framework, we applied the ab initio HF method to several nanosized graphite sheets. We considered the fundamental graphite sheet **1** and relevant graphite sheets **3b** and **5** that show significant heteroatomic effects. Computed transfer coefficients

TABLE 3: Computed Transfer Coefficients and Energy Gaps Obtained by HF/6-31G(d) in $C_{72}H_{26}$ (1), $C_{70}B_2H_{26}$ (3b), and $C_{68}N_4H_{26}$ (5)

	$T(E_F)$ (10^{-6})					
molecule	$T_{11'}$	$T_{22'}$	$T_{33'}$	$T_{55'}$	$T_{55''}$	E_g (eV)
1	7.47	1.86	0.18	0.98	0.02	7.27
3b	286.94	14.81	0.88	1.07	0.13	5.87
5	66.91	1.62	0.06	23.45	0.28	3.03

are listed in Table 3. Because the HOMO, HOMO − 1, LUMO, and LUMO + 1 in **1** obtained from ab initio HF calculations are essentially identical with those from PPP calculations, $T_{11'}$ is the largest transfer coefficient in **1**, and the relationships in magnitude among $T_{11'}$, $T_{22'}$, and $T_{33'}$ are same as those obtained within the PPP framework. The HOMO (LUMO) pattern obtained from ab initio HF and PPP calculations are similar in **3b**, and thus significant heteroatomic effect is provided in $T_{11'}$ in **3b** in analogy with the discussion within the PPP framework. On the other hand, although a significant heteroatomic effect in **5** is obtained in $T_{11'}$, the way of connection leading to the largest transfer coefficient is not consistent with that found in the PPP framework. $T_{11'}$ in **5** is the largest transfer coefficient within the ab initio HF framework, while $T_{55''}$ in **5** is the largest within the PPP framework (see Table 2). This is due to a change in the order of frontier orbitals in **5** in the two calculations. The HOMO (LUMO) in **5** obtained with the ab initio HF method corresponds to the HOMO − 1 (HOMO) shown in Figure 4. According to rules I and II, we predict that $T_{11'}$ in **5** is the most significant transfer coefficient within the ab initio HF framework, and the result of computed transfer coefficients in **5** is, in fact, in good agreement with the prediction.

Conclusions

We found important rules for effective quantum transport in various nanosized graphite sheets by using the Caroli−Combescot−Landauer formulation within the PPP and the ab initio HF frameworks. The rules are summarized as follows: (I) the MO coefficients at two atoms connected with metallic leads must be large in the frontier orbitals (the HOMO and LUMO or other MOs in the vicinity of the Fermi energy); (II) the product of MO expansion coefficients at the two atoms in the HOMO must be different in sign from that in the LUMO, and the product of MO expansion coefficients at the two atoms in the HOMO (LUMO) should be same in sign with that in occupied (unoccupied) MOs in the vicinity of the Fermi energy. In the calculations of nanosized graphite sheets that involve B, N, and O atoms, we confirmed significant heteroatomic effects in quantum transport. Heteroatoms can localize the electronic density of the HOMO and LUMO at certain sites, and therefore, quantum transport effects are significantly enhanced. According to the two rules that we derived, effective ways of connection are readily predicted by looking at MOs calculated with an appropriate MO method.

Acknowledgment. K.Y. acknowledges Grants-in-aid for Scientific Research from the Ministry of Culture, Sports, Science and Technology of Japan (MEXT), the Japan Society for the Promotion of Science, and the Murata Science Foundation for their support of this work. A part of this work is supported by Kyushu University P & P "Green Chemistry" and "Nanotechnology Support Project" of MEXT. Computations were in part carried out at the Computer Center of the Institute for Molecular Science.

References and Notes

(1) Aviram, A.; Ratner, M. A. *Chem. Phys. Lett.* **1974**, *29*, 277.
(2) Landauer, R. *IBM J. Res. Dev.* **1957**, *1*, 223.
(3) Magoga, M.; Joachim, C. *Phys. Rev. B* **1997**, *56*, 4722.
(4) Mujica, V.; Kemp, M.; Roitberg, A.; Ratner, M. *J. Chem. Phys.* **1996**, *104*, 7296.
(5) Seminario, J. M.; Zacarias, A. G.; Tour, J. M. *J. Phys. Chem. A* **1999**, *103*, 7883.
(6) Gutierrez, R.; Fagas, G.; Cuniberti, G.; Grossmann, F.; Schmidt, R.; Richter, K. *Phys. Rev. B* **2002**, *65*, 113410.
(7) Paulsson, M.; Stafström, S. *Phys. Rev. B* **2001**, *64*, 035416.
(8) Tian, W.; Datta, S.; Hong, S.; Reifenberger, R.; Henderson, J. I.; Kubiak, C. P. *J. Chem. Phys.* **1998**, *109*, 2874.
(9) Nardelli, M. B. *Phys. Rev. B* **1999**, *60*, 7828.
(10) Choi, H. J.; Ihm, J.; Louie, S. G.; Cohen, M. L. *Phys. Rev. Lett.* **2000**, *84*, 2917.
(11) Hey, R.; Schreiber, M. *J. Chem. Phys.* **1995**, *103*, 10726.
(12) Hansson, A.; Paulsson, M.; Stafström, S. *Phys. Rev. B* **2000**, *62*, 7639.
(13) Cheong, A.; Roitberg, A. E.; Mujica, V.; Ratner, M. A. *J. Photochem. Photobiol. A: Chem.* **1994**, *82*, 81.
(14) Tada, T.; Yoshizawa, K. *ChemPhysChem* **2002**, *3*, 1035.
(15) (a) Hess, B. A., Jr.; Schaad, L. J. *J. Am. Chem. Soc.* **1971**, *93*, 305. (b) Hess, B. A., Jr.; Schaad, L. J. *J. Org. Chem.* **1971**, *36*, 3418.
(16) (a) Herndon, W. C. *Tetrahedron* **1973**, *29*, 3. (b) Herndon, W. C.; Ellzey, M. L. *J. Am. Chem. Soc.* **1974**, *96*, 6631. (c) Herndon, W. C. *J. Org. Chem.* **1975**, *40*, 3583. (d) Herndon, W. C. *J. Org. Chem.* **1981**, *46*, 2119. (e) Herndon, W. C. *Tetrahedron* **1982**, *38*, 1389.
(17) (a) Stein, S. E.; Brown, R. L. *Carbon* **1985**, *23*, 105. (b) Stein, S. E.; Brown, R. L. *J. Am. Chem. Soc.* **1987**, *109*, 3721. (c) Chen, R. H.; Kafafi, S. A.; Stein, S. E. *J. Am. Chem. Soc.* **1989**, *111*, 1418. (d) Stein, S. E.; Brown, R. L. *J. Am. Chem. Soc.* **1991**, *113*, 787. (e) Stein, S. E. *Acc. Chem. Res.* **1991**, *24*, 350.
(18) Klimkâns, A.; Larsson, S. *Chem. Phys.* **1994**, *189*, 25.
(19) (a) Yamabe, T.; Yamashita, S.; Yamabe, H.; Fukui, K.; Tanaka, K. *Collect. Czech. Chem. Commun.* **1988**, *53*, 1881. (b) Yoshizawa, K.; Okahara, K.; Sato, T.; Tanaka, K.; Yamabe, T. *Carbon* **1994**, *32*, 1517. (c) Yoshizawa, K.; Yahara, K.; Tanaka, K.; Yamabe, T. *J. Phys. Chem. B* **1998**, *102*, 498.
(20) Nakada, K.; Fujita, M.; Dresselhaus, G.; Dresselhaus, M. S. *Phys. Rev. B* **1996**, *54*, 17954.
(21) (a) Iyer, V. S.; Wehmeier, M.; Brand, J. D.; Keegstra, M. A.; Müllen, K. *Angew. Chem., Int. Ed. Engl.* **1997**, *36*, 1604. (b) Müller, M.; Iyer, V. S.; Kübel, C.; Enkelmann, V.; Müllen, K. *Angew. Chem., Int. Ed. Engl.* **1997**, *36*, 1607. (c) Weiss, K.; Beernink, G.; Dötz, F.; Birkner, A.; Müllen, K.; Wöll, C. H. *Angew. Chem., Int. Ed.* **1999**, *38*, 3748. (d) Beernink, G.; Gunia, M.; Dötz, F.; Öström, H.; Weiss, K.; Müllen, K.; Wöll, C. *ChemPhysChem* **2001**, *2*, 317. (e) Simpson, C. D.; Brand, J. D.; Beeresheim, A. J.; Przybilla, L.; Räder, H. J.; Müllen, K. *Chem.—Eur. J.* **2002**, *8*, 1424.
(22) (a) Pariser, R.; Parr, R. G. *J. Chem. Phys.* **1953**, *21*, 767. (b) Pople, J. A. *Trans. Faraday Soc.* **1953**, *49*, 1375.
(23) (a) Caroli, C.; Combescot, R.; Nozieres, P.; Saint-James, D. *J. Phys. C* **1971**, *4*, 916. (b) Combescot, R. *J. Phys. C* **1971**, *4*, 2611.
(24) (a) Hinze, J.; Jaffe, H. H. *J. Am. Chem. Soc.* **1962**, *84*, 540. (b) Dewar, M. J. S.; Morita, T. *J. Am. Chem. Soc.* **1969**, *91*, 796. (c) Murrell, J. N.; Harget, A. J. *Semiempirical self-consistent-field molecular orbital theory of molecules*; Wiley-Interscience: London, New York, 1972.
(25) Wolfsberg, M.; Helmholz, L. *J. Chem. Phys.* **1952**, *20*, 837.
(26) Papaconstantopoulos, D. A. *Handbook of the Band Structure of Elemental Solids*; Plenum: New York, 1986.
(27) These parameters were estimated by the extended Hückel method in the case where the interatomic distances are 2.5 Å. The parameters are resonance integrals between the 6s atomic orbital in Au and 2p π atomic orbitals.
(28) Dewar, M. J. S.; Zoebisch, E. G.; Healy, E. G.; Stewart, J. J. P. *J. Am. Chem. Soc.* **1985**, *107*, 3902.
(29) Frisch, M. J.; Trucks, G. W.; Schlegel, H. B.; Scuseria, G. E.; Robb, M. A.; Cheeseman, J. R.; Zakrzewski, V. G.; Montgomery, J. A., Jr.; Stratmann, R. E.; Burant, J. C.; Dapprich, S.; Millam, J. M.; Daniels, A. D.; Kudin, K. N.; Strain, M. C.; Farkas, O.; Tomasi, J.; Barone, V.; Cossi, M.; Cammi, R.; Mennucci, B.; Pomelli, C.; Adamo, C.; Clifford, S.; Ochterski, J.; Petersson, G. A.; Ayala, P. Y.; Cui, Q.; Morokuma, K.; Malick, D. K.; Rabuck, A. D.; Raghavachari, K.; Foresman, J. B.; Cioslowski, J.; Ortiz, J. V.; Stefanov, B. B.; Liu, G.; Liashenko, A.; Piskorz, P.; Komaromi, I.; Gomperts, R.; Martin, R. L.; Fox, D. J.; Keith, T.; Al-Laham, M. A.; Peng, C. Y.; Nanayakkara, A.; Gonzalez, C.; Challacombe, M.; Gill, P. M. W.; Johnson, B. G.; Chen, W.; Wong, M. W.; Andres, J. L.; Head-Gordon, M.; Replogle, E. S.; Pople, J. A. *Gaussian 98*; Gaussian, Inc.: Pittsburgh, PA, 1998.
(30) Fukui, K. *Theory of Orientation and Stereoselection*; Springer: Heidelberg, Germany, 1970.
(31) Woodward, R. B.; Hoffmann, R. *The Conservation of Orbital Symmetry*; Chemie, GmbH: Weinheim, Germany, 1970.